

## Reliable and flexible carbon-nanofiber-based all-plastic field emission devices

H. S. Sim, S. P. Lau,<sup>a)</sup> H. Y. Yang, and L. K. Ang

School of Electrical and Electronic Engineering, Nanyang Technological University, Singapore 639798, Singapore

M. Tanemura and K. Yamaguchi

Graduate School of Engineering, Nagoya Institute of Technology, Gokiso-cho, Showa-ku, Nagoya 466-8555, Japan

(Received 19 January 2007; accepted 1 March 2007; published online 2 April 2007)

The authors present the fabrication and electrical characterization of carbon nanofiber-based flexible field emitters prepared by an ion beam technique. The flexible emitters are extremely robust under various stress conditions and show no sign of degradation after 16 h long lifetime test. An all-plastic flexible field emission device with excellent emission properties has also been demonstrated using phosphor-coated polyester as an anode. © 2007 American Institute of Physics.

[DOI: 10.1063/1.2719239]

Carbon nanofibers (CNFs) have attracted much attention because of their unique physical properties that are suitable for a wide range of potential applications such as field emitter.<sup>1</sup> The advantages of CNF field emitter are low field emission threshold, high aspect ratio, good chemical stability, and excellent mechanical strength.<sup>2–4</sup> Traditionally, field emitters were constrained to grow on substrate that can withstand high temperatures due to the high processing temperature required.<sup>1</sup> In recent years, several research groups have been involved in the growing of carbon nanostructures on plastic substrates for flexibility purposes, using plasma-enhanced chemical vapor deposition,<sup>5</sup> solution-based method,<sup>6</sup> electrophoretic method,<sup>7</sup> and ion beam method.<sup>8</sup> However, the ion beam method is exploited here, as it can produce aligned CNFs on any substrates with relatively large area ( $>28\text{ cm}^2$ ) at room temperature. The advantages of flexible substrate, among many, are lower cost of producing the emitter and allowing emitter of any geometry and shape to be made for use in field emission applications.<sup>9</sup> However, the field emission characteristics and the reliability of flexible field emitter under various stressing conditions remain unexplored. In this letter, we demonstrate an all-plastic flexible field emission device and study the reliability of the flexible CNF field emitters under substantial bending conditions. The ability to grow reliable CNFs on low-cost flexible substrates may open up numerous fields of applications such as x-ray radiotherapy<sup>9–11</sup> and “rollable” field emission displays.

CNFs were grown on  $140\text{ }\mu\text{m}$  thick commercially available Kapton polyimide foils. For the synthesis of CNFs, carbon film was first coated onto the polyimide film. The carbon-coated polyimide substrate was then bombarded with obliquely incident  $\text{Ar}^+$  using Kaufman-type ion gun (Iontech. Inc. Ltd., model MPS 3000 FC) at a low vacuum pressure of  $1.5 \times 10^{-5}\text{ Pa}$ . The diameter of the ion gun was 6 cm and the energy of the beam employed was 1 kV. The incidence angle was  $45^\circ$  from the normal to the surface, and the carbon-coated polyimide substrate was irradiated at room temperature for 60 min.

Figure 1(a) shows the scanning electron microscopy (SEM) micrograph of the emitter arrays consisting of CNF-tipped conelike nanostructures. The conical protrusions are abundant and uniformly distributed, the length of the CNF ranging from  $0.5$  to  $1\text{ }\mu\text{m}$ , while the diameter is estimated at around  $200\text{--}500\text{ nm}$ . The CNF structure grown on conical bases is advantageous as each individual CNF was spaced at a distance much more than its length between adjacent fibers, therefore minimizing or diminishing screening effect.<sup>12</sup> The transmission electron microscopy (TEM) micrograph shows an individual CNF, which measured approximately  $15\text{ nm}$  in diameter [Fig. 1(b)]. The electron diffraction pattern of the corresponding CNF reveals the amorphous nature of the CNF. Figure 1(c) illustrates the growth mechanism of the CNF. The first step is to induce the nano- to micro-sized surface protrusions on the carbon-coated surfaces by ion bombardments at  $45^\circ$ . The conditions of the protrusions can also be controlled by enhancing the surface texture using oblique sputtering (i.e., by focusing the ion beam at an angle). The protrusions were formed by the redeposition of sputter ejected carbon atoms from the surface onto the sidewall of the conical protrusions. These carbon atoms can then diffuse toward the tips during sputtering. The surface diffusion is

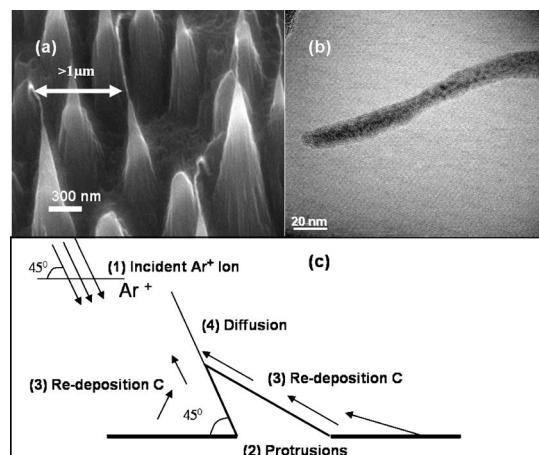


FIG. 1. (a) High magnification SEM micrograph showing an individual ultrafine CNF. (b) TEM image of a single CNF. (c) Schematic representation of the growth mechanism of ion-induced CNFs.

<sup>a)</sup> Author to whom correspondence should be addressed; electronic mail: esplau@ntu.edu.sg

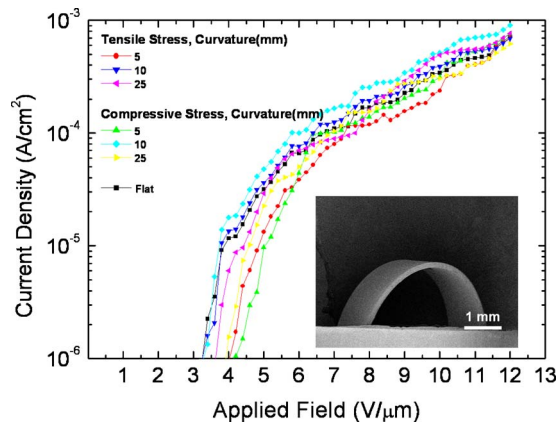


FIG. 2. (Color online) Field emission measurement of the flexible CNF emitters at different bending curvatures, inset showing a bended flexible CNF field emission device.

thought to be the reason for the ion-induced CNF growth.

In order to measure the field emission properties of the flexible CNF emitters under various bending conditions, an adhesive copper conducting tape (3 M) was used as the anode, with thickness of  $100\ \mu\text{m}$  and separated by a  $100\ \mu\text{m}$  polytetrafluorethylene (PTFE) spacer. The copper tape, the spacer, and the polyimide CNF film are cut to the same dimensions to form a  $1.0 \times 2.0\ \text{cm}^2$  flexible field emitter device. A hole of 6 mm was punched through the spacer and, hence, the test exposed emission area was  $0.28\ \text{cm}^2$ . The same device was bent to different curvatures and directions (i.e., inward or outward bending for tensile or compressive stress, respectively). Three different cylindrical structures of diameters 10, 25, and 50 mm were employed in the field emission experiments. Field emission measurements were carried out in a parallel plate configuration at a base pressure of  $10^{-6}\ \text{Pa}$  with applied voltages sweeping from 0 to 1100 V. Figure 2 illustrates the field emission characteristics of the samples under various bending conditions. The threshold field of the emitter at flat condition (or no bending) was approximately  $3.2\ \text{V}/\mu\text{m}$ , whereas the threshold fields for emitter under various stressing conditions changed slightly from 3.1 to  $4.2\ \text{V}/\mu\text{m}$  for a current density of  $1\ \mu\text{A}/\text{cm}^2$ . The average threshold field for all the conditions is  $\sim 3.65\ \text{V}/\mu\text{m}$ . This is comparable to carbon nanotubes grown on polyimide substrate and CNFs grown on the graphite plate.<sup>5,13</sup> No hystericlike behavior is observed on the curves and no remarkable changes in the threshold field can be observed under different bending curvatures for both tensile and compressive stressed emitters. These facts imply that stresses do not have significant effect on the threshold field of the CNF emitters. The SEM image of a bended flexible CNF emitter (radius of curvature=2 mm) is shown in the inset of Fig. 2. The excellent adhesion of the CNFs on the polyimide is manifest even under severe bending conditions suggesting that the CNF is robust and tough, suitable for use in practical field emission devices. Indeed, the same device has been bent in various conditions for many times and no noticeable changes in the field emission properties can be observed.

For estimation of the field enhancement, the emission data were analyzed using a Fowler-Nordheim plot by applying the equation

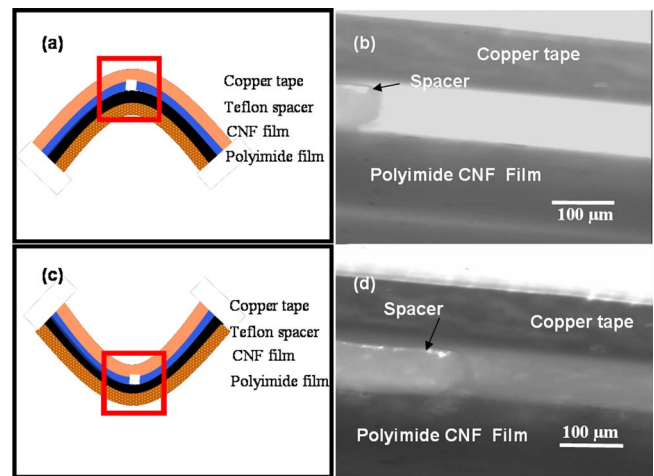


FIG. 3. (Color online) (a) and (b) are the schematic diagrams of the device under tensile stress and optical microscope image of the gap distance as indicated by the “box,” respectively. (c) and (d) are the schematic diagrams of the device under compressive stress and the corresponding optical images of the gap distance, respectively.

$$J = \frac{aF^2}{\beta^2\phi} \exp\left(\frac{-b\phi^{3/2}}{\beta F}\right), \quad (1)$$

where  $J$  is the current density ( $\text{A}/\text{m}^2$ ),  $F$  is the electric field at the tip apex,  $\phi$  is the work function,  $\beta$  is the field enhancement factor, and  $a$  and  $b$  are both constants.<sup>2</sup> This may also be expressed as  $F = \beta(V/d)$ , where  $V$  is the applied potential and  $\beta$  is the field enhancement factor, which may be expressed as  $\beta = h/r$ , where  $h$  is the height of the tip and  $r$  is the radius of curvature of the tip apex. Thus, the values of the field enhancement factor could then be estimated from the slope of the Fowler-Nordheim plot by assuming a work function of 4.5 eV for CNFs. From the equation, it is important to make the tips as sharp as possible in order to reduce the field required for emission. The typical field enhancement value obtained for the flat emitter is around 2500, which is comparable with the field enhancement reported on CNFs grown on a graphite plate.<sup>13</sup> The high field enhancement value obtained could be due to the high aspect ratio of the ultrafine long CNF.

For stable field emission, good adhesion is required between the base substrate and emitters as any field strong enough that exerted on the CNFs during field emission can peel off the CNFs from the substrates, causing current decay and arcing.<sup>14</sup> As shown in Fig. 1, the CNFs are uniformly distributed. The work function and aspect ratio of CNFs are assumed to be uniform throughout the emitted area. It is hence important to check the gap between the anode and cathode of the flexible CNF emitter under various bending conditions in order to appreciate the results obtained earlier. Consequently, the gap distance between the copper anode and the CNF polyimide film separated by a  $100\ \mu\text{m}$  spacer was measured using a Nikon optical measuring microscope mm-40. A small gap of  $5 \times 3\ \text{mm}^2$  was made on top of the PTFE spacer rather than the usual  $0.28\ \text{cm}^2$  hole made at the center, so that a gap was observed between the cathode (CNF film) and anode (copper tape) when viewed in cross section. The flexible emitter was then fixed onto a 25 mm cylindrical structure and observed by the optical microscope. Figures 3(a) and 3(b) are the schematic diagrams of the devices under tensile and compressive stress conditions, respectively.

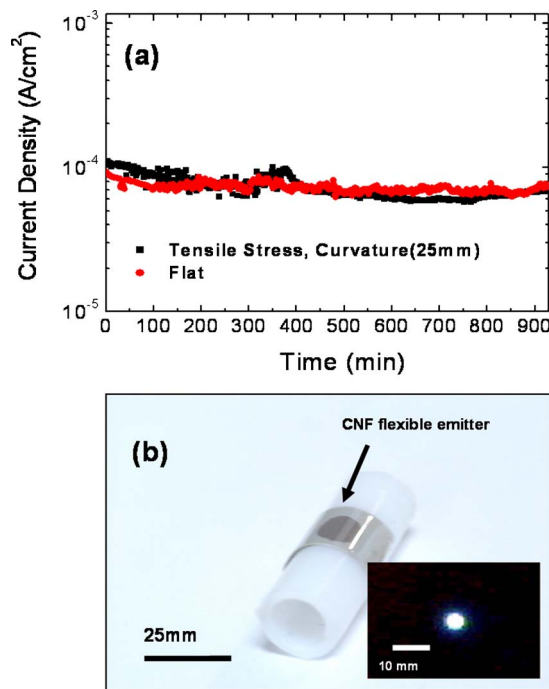


FIG. 4. (Color online) (a) Field emission stability as a function of time at an applied field of  $10 \text{ V}/\mu\text{m}$  for flat and tensile stressed ( $r=25 \text{ mm}$ ) emitter for a period of 16 h. (b) Photograph of the all-plastic field emission device mounted on a 25 mm diameter structure. The inset shows the emission spots captured from the phosphor-coated plastic substrate at an applied field of  $13 \text{ V}/\mu\text{m}$ .

The corresponding cross-sectional views of the flexible emitter at both conditions are shown in Figs. 3(c) and 3(d). The average gap distances obtained for several measurements were around  $100.5 \mu\text{m} \pm 10\%$  and  $99 \mu\text{m} \pm 9\%$  for tensile and compressive stressed samples, respectively. These deviations at the gap differences at various points, therefore, accounted for the minor change of threshold fields achieved earlier. If we considered the average threshold fields of around  $3.65 \text{ V}/\mu\text{m}$  for different stressing conditions at a 10% discrepancy in emitter to anode distance, the calculated threshold field variations will range from 3.3 to  $4.1 \text{ V}/\mu\text{m}$ , which is consistent with what we obtained from the experimental results. This implies that keeping consistent gap distance between anode and cathode of the flexible emitter is the key to a stable field emission. The fluctuations of threshold field of roughly 10% is mainly due to the variations of gap distances between the anode and cathode, of the flexible emitter. As the anode, cathode, and insulation spacer were made from different materials, thus creating an emitter structure having different Young's moduli, the bending between respective materials were different when a force was applied to the emitter structure. This discrepancy can be minimized by choosing materials with comparable Young's moduli and properly securing the anode, the insulation spacer, and the cathode.

The emitter was subjected to a reliability test, and a field of  $10 \text{ V}/\mu\text{m}$  was applied to the emitter in flat and stressed conditions for a duration of 16 h, as shown in Fig. 4(a). The average current densities of the emitter under unstressed and tensile stressed conditions were measured to be around  $7.25 \times 10^{-5}$  and  $7.11 \times 10^{-5} \text{ A}/\text{cm}^2$ , respectively. The degradation of current densities at both conditions were low and well maintained at around  $7.18 \times 10^{-5} \text{ A}/\text{cm}^2$  after 16 h of

emission testing. The emitter is indeed very robust regardless of planar or bended conditions. In order to demonstrate the feasibility of constructing an all-plastic flexible field emission display (APFED), a ZnS:Ag phosphor-coated polyester sheet (Eljen Technology) of  $250 \mu\text{m}$  thickness was used as a flexible anode, with a central emission wavelength of 450 nm. The phosphor on plastic substrate is meant for ionization ion detection such as alpha particles, thus the light efficiency for electron is low. The anode has to be conductive in order to attract electrons from the emitter, thus a thin layer of 10 nm Pt was deposited onto the phosphor. This conductive layer must not be too thick as the field electrons might not be able to penetrate through the Pt layer and bombard the phosphor layer. Figure 4(b) shows the APFED mounted onto a cylindrical object (radius=25 mm) with an emission area of  $0.28 \text{ cm}^2$ . The emission area of the APFED was captured by a charge-coupled device camera with an applied field of  $5\text{--}13 \text{ V}/\mu\text{m}$ , showing fairly uniform emission as shown in the inset of Fig. 4(b). The concept of APFED may open up opportunities in future "rollable" display that is lightweight, flexible (i.e., can be made to whatever shape for better viewing angles), and of high resolution (i.e., nanosized pixels are possible with CNF tips).

In summary, an all-plastic field emission display with excellent field emission properties has been demonstrated using CNFs as field emitters. The flexible CNF field emitters are robust and reliable under various stress conditions and severe lifetime test.

This work was partly supported by the Agency for Science, Technology and Research of Singapore (Project No. 0221010020), NTU RGM 17/04, the Japan Society for the Promotion of Science (JSPS; Grants-in-Aid for Scientific Research B, No. 15360007), and the NITECH 21st Century COE Program "World Ceramics Center for Environmental Harmony." One of the authors (H.Y.Y.) acknowledges the support of Singapore Millennium Foundation Fellowships.

<sup>1</sup>A. V. Melechko, V. I. Merkulov, T. E. McKnight, M. A. Guillorn, K. L. Klein, D. H. Lowndes, and M. L. Simpson, *J. Appl. Phys.* **97**, 041301 (2005).

<sup>2</sup>W. Zhu, C. Bower, O. Zhou, G. Kochanski, and S. Jin, *Appl. Phys. Lett.* **75**, 873 (1999).

<sup>3</sup>V. I. Merkulov, D. H. Lowndes, and L. R. Baylor, *Appl. Phys. Lett.* **75**, 1228 (1999).

<sup>4</sup>K. B. K. Teo, M. Chhowalla, G. A. J. Amaratunga, W. I. Milne, G. Pirio, P. Legagneux, F. Wyczisk, D. Pribat, and D. G. Hasko, *Appl. Phys. Lett.* **80**, 2011 (2002).

<sup>5</sup>S. Hofmann, C. Ducati, B. Kleinsorge, and J. Robertson, *Appl. Phys. Lett.* **83**, 4661 (2003).

<sup>6</sup>J. H. Choi, J. H. Park, and J. S. Moon, *Diamond Relat. Mater.* **15**, 44 (2006).

<sup>7</sup>Huizhong Ma, Lan Zhang, Junjie Zhang, Liwei Zhang, Ning Yao, and Binglin Zhang, *Appl. Surf. Sci.* **251**, 258 (2005).

<sup>8</sup>M. Tanemura, T. Okita, H. Yamauchi, and S. Tanemura, *Appl. Phys. Lett.* **85**, 3831 (2004).

<sup>9</sup>T. T. Tan, H. S. Sim, S. P. Lau, H. Y. Yang, M. Tanemura, and J. Tanaka, *Appl. Phys. Lett.* **88**, 103105 (2006).

<sup>10</sup>G. Z. Yue, Q. Qiu, B. Cao, Y. Cheng, J. Zhang, H. Shimasa, S. Chang, J. P. Lu, and O. Zhou, *Appl. Phys. Lett.* **81**, 355 (2002).

<sup>11</sup>Y. B. Zhang, S. P. Lau, L. Huang, and M. Tanemura, *Appl. Phys. Lett.* **86**, 123115 (2005).

<sup>12</sup>L. Nilsson, O. Groening, C. Emmenegger, O. Kuettel, E. Schaller, and L. Schlappbach, *Appl. Phys. Lett.* **76**, 2071 (2000).

<sup>13</sup>M. Tanemura, J. Tanaka, K. Itoh, T. Okita, L. Miao, and S. Tanemura, *Appl. Phys. Lett.* **87**, 193102 (2005).

<sup>14</sup>L. Nilsson, O. Groening, P. Groening, and L. Schlappbach, *Appl. Phys. Lett.* **79**, 1036 (2001).